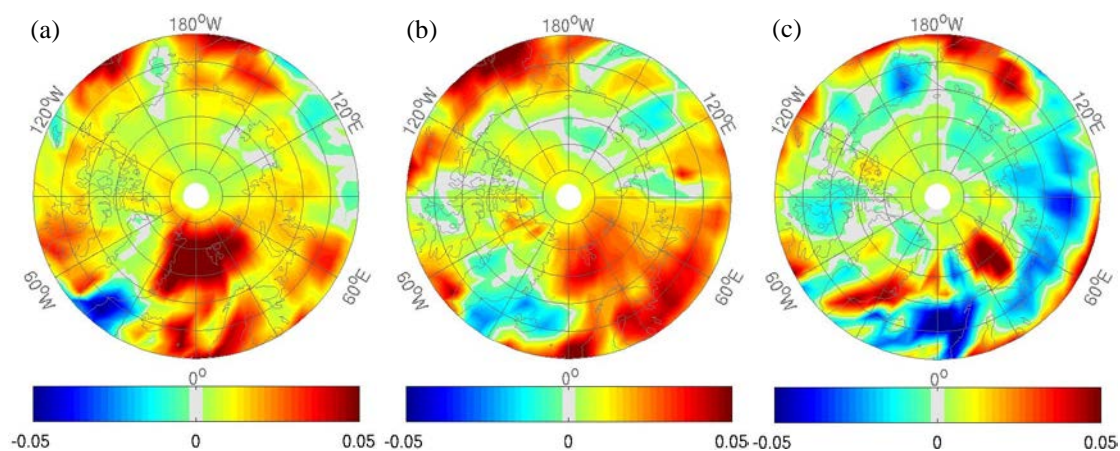


## Supplementary material

**Table S1** Information of 12 CMIP5 climate models used in this study. The spatial resolution of atmosphere is expressed by the number of longitudinal grid cells  $\times$  the number of latitudinal grid cells.

Model	Institute/Country	Spatial resolution of atmosphere
GFDL-CM3	NOAA GFDL/USA	144 $\times$ 90
GFDL-ESM2G	NOAA GFDL/USA	144 $\times$ 90
GFDL-ESM2M	NOAA GFDL/USA	144 $\times$ 90
GISS-E2-H	NASA GISS/USA	144 $\times$ 90
GISS-E2-R	NASA GISS/USA	144 $\times$ 90
HadGEM2-AO	MOHC/UK	192 $\times$ 145
HadGEM2-ES	MOHC/UK	192 $\times$ 145
MIROC5	MIROC/Japan	256 $\times$ 128
MIROC-ESM	MIROC/Japan	128 $\times$ 64
MIROC-ESM-CHEM	MIROC/Japan	128 $\times$ 64
MRI-CGCM3	MRI/Japan	320 $\times$ 160
NorESM1-ME	NCC/Norway	144 $\times$ 96

5



**Figure S1.** Spatial pattern of differences in annual hydroclimate between MCA (950-1250) and LIA (1450-1850) based on (a) HadCM3, (b) IPSL-CM5A-LR and (c) MPI-ESM-P last-millennium simulations. The values are the standardized annual total precipitation.

20

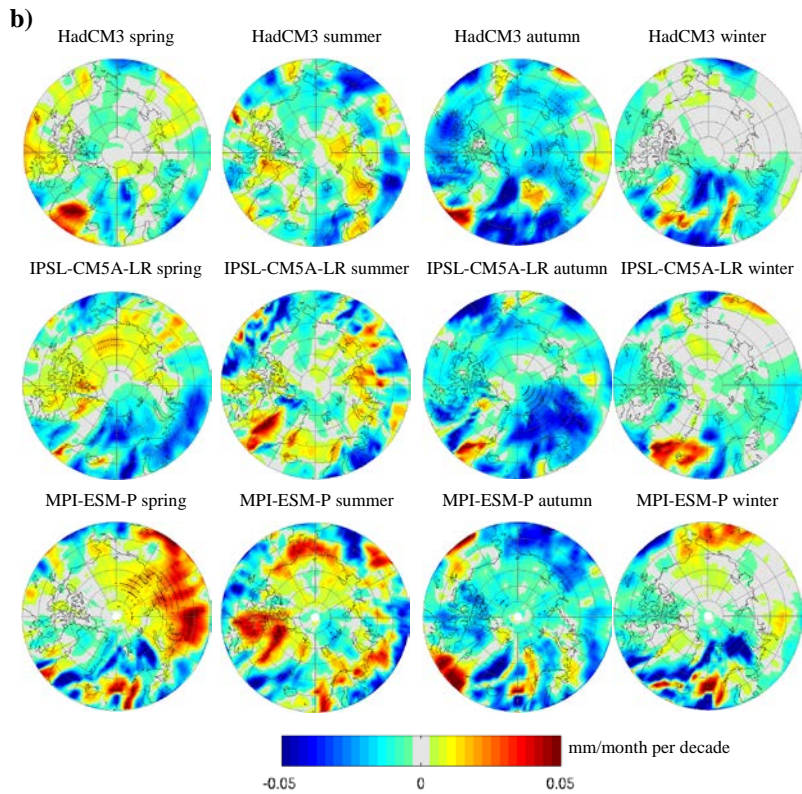
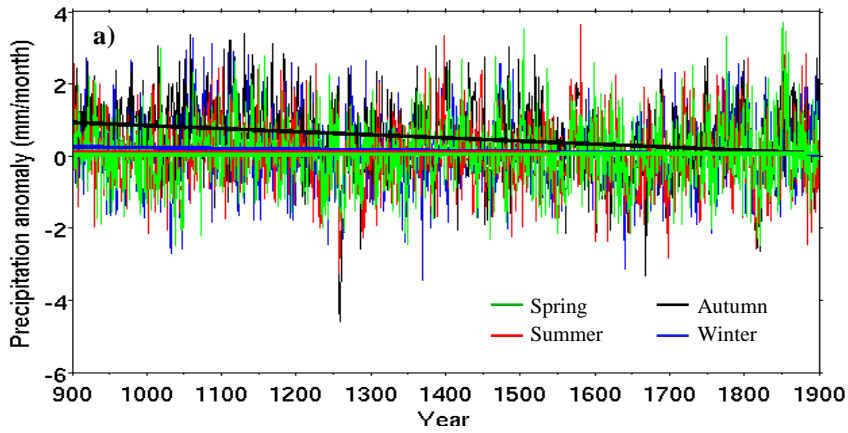


**Figure S2.** a) Variability and linear trends of the Arctic spring, summer, autumn and winter total precipitation anomalies (900-1900 CE) from 3-model (HadCM3, IPSL-CM5A-LR and MPI-ESM-P) ensemble mean. b) Spatial patterns of linear trends in seasonal total precipitation anomalies over (900-1850 CE) from 3 climate models. Dots mark grids where the trend is significant ( $p < 0.01$ ).